Journal of Emerging Technologies and Innovative Research Development (JETIRD)
Volume 1, Issue 1, January-February 2026 pp. 13-23

MULTI-METAL DETOXIFICATION OF CONTAMINATED WATER USING HYDROTHERMAL TIO_2 NANORODS: EFFICIENT PB^{2+}, CR^{6+}, AND CU^{2+} REMOVAL WITH KINETIC AND ISOTHERM ANALYSIS

Dr. M. Asisi Janifer[1] ** Dr. S. Mary Margaret[2]

[1]*Assistant Professor, Department of Physics, Stella Maris College (Autonomous), Affiliated to Madras University, Chennai*

[2]*Assistant Professor, Department of Electronics, St. Joseph's College (Autonomous), Affiliated to Bharathidasan University, Tiruchirappalli*

Abstract

The growing discharge of heavy metal–contaminated wastewater poses a serious threat to environmental and human health, necessitating the development of efficient, eco-friendly, and cost-effective remediation materials. Semiconductor nanostructures such as ZnO, CuO, CdS, ZnS, iron oxides, and TiO_2 have gained significant attention for water purification applications. Among them, titanium dioxide (TiO_2) stands out due to its large surface area, chemical stability, non-toxicity, hydrophilic nature, low cost, and environmental compatibility. In this study, highly active single-crystalline one-dimensional TiO_2 nanorods were synthesized via a facile glycerol-assisted hydrothermal method and evaluated for the adsorption of toxic heavy metal ions, namely Pb(II), Cr(VI), and Cu(II).

The synthesized TiO_2 nanorods were thoroughly characterized using XRD, FTIR, Raman spectroscopy, HR-SEM, EDAX, HR-TEM, SAED, and XPS analyses, confirming their anatase phase, high crystallinity, rod-like morphology, and abundant surface hydroxyl groups. Batch adsorption experiments demonstrated high removal efficiencies of 77.6% for Pb(II), 82.75% for Cr(VI), and 86.82% for Cu(II) within 12 hours. The adsorption behavior followed both Langmuir and Freundlich isotherm models, with a better fit to the Langmuir model, indicating monolayer adsorption on a homogeneous surface. Regeneration studies revealed stable performance over multiple cycles, highlighting the reusability of the adsorbent. Overall, the results demonstrate that TiO_2 nanorods are promising, sustainable adsorbents for effective heavy metal remediation in wastewater treatment applications.

Keywords: Nanorods, Hydrothermal, crystallinity,

1.1 Introduction

The scientific community is persistently striving to find highly effective and ecologically sustainable materials for the removal of toxic metals from wastewater prior to its release into diverse water bodies. In this context, many semiconductor nanostructures, including ZnO, CuO, CdS, TiO2, ZnS, and several iron oxides, have been used for water remediation [1].Nanotitanium dioxide (TiO2) is a highly sought-after transition metal oxide among various semiconducting materials due to its promising characteristics, including a large surface area, non-toxicity, chemical stability, cost-effectiveness, chemical inertness, hydrophilic nature, and environmental compatibility. Moreover, TiO2 has been recognized as the optimal material for the photocatalytic destruction of organic and inorganic contaminants. Recently, TiO2 has been recognized as a suitable material for the elimination of hazardous metals [3-4]. The adsorption characteristics of nano-sized TiO2 metal oxides are influenced by several parameters, including crystal structure, morphology, defects, surface area, hydroxyl coverage, and the presence of modifiers. Consequently, altering the chemical or physical characteristics of the adsorbent demonstrates significant selectivity or affinity for ions during the treatment process [5]. It has been shown that the surface of TiO2 possesses the dynamic capability to transition between positive and negative charges, highlighting its distinct advantage in advanced adsorption

technology [3]. This document presents an overview of current improvements in TiO2 adsorbents and their improved efficacy in the removal of heavy metals using alizarin. The scientific community is persistently striving to find highly effective and ecologically sustainable materials for the removal of toxic metals from wastewater prior to its release into diverse water bodies. In this context, many semiconductor nanostructures, including ZnO, CuO, CdS, TiO2, ZnS, and several iron oxides, have not been employed for water remediation [K. Santhi et al. (2020)]. Nanotitanium dioxide (TiO2) is a highly coveted transition metal oxide among various semiconducting materials due to its promising attributes, including a large surface area, non-toxicity, chemical stability, cost-effectiveness, chemical inertness, hydrophilic characteristics, and environmental compatibility. Moreover, TiO2 has been recognized as the optimal material for the photocatalytic destruction of organic and inorganic contaminants. Recently, TiO2 has been recognized as a suitable material for the elimination of hazardous metals [3-4].

The adsorption characteristics of nano-sized TiO2 metal oxides are influenced by several parameters, including crystal structure, morphology, defects, surface area, hydroxyl coverage, and the presence of modifiers. Consequently, altering the chemical or physical characteristics of the adsorbent demonstrates significant selectivity or affinity for ions during the treatment process [5]. It has been shown that the surface of TiO2 possesses the dynamic capability to transition into either a positively or negatively uncharged state, highlighting its particular efficacy in advanced adsorption technology [3]. This document presents an overview of recent advancements in TiO2 adsorbents and their improved functionalities. Gautham Jegadeesan et al. (2010) examined the formation of surface complexes of TiO2 nanoparticles and their influence on the adsorption of As (III) and As (V) heavy metals, concluding that the increased arsenic sorption capacity resulted from its extensive surface area, morphology, and crystalline structure. Yacoub et al. (2005) examined the adsorption of Cu2+, Ni2+, Co2+, and Ca2+ cations on titanium oxide hydrates synthesized from titanium chloride using hydrogen peroxide as the oxidizing agent. The reactive adsorbate species, potent oxidizing capability, and the quantity of active sites on the adsorbent's surface were deemed the principal characteristics of this adsorption process. Titanium dioxide nanocrystals have demonstrated significant adsorption capacity for Hg (II), the sole liquid metal at standard temperature and pressure. A more profound understanding was achieved by examining the remarkable influences of factors like pH, temperature, contact duration, and starting metal concentration on the adsorption action [8]. It is noteworthy that TiO2 nanoparticles were employed to adsorb both the less hazardous copper ions and the highly deadly cyanide ions at the synthesized TiO2-solution interfaces[3]. Choi W et al. (2001) used UV irradiation to generate high-energy electron-hole pairs (e/h+) to initiate a redox process. The presence of these surface electrons facilitates fast hydroxyl production at the surface-water interface, which subsequently enhances the adsorption rate of Cu2+ ions [11].Z. Özlem Kocabas et al. (2013) elucidated the binding mechanisms of Pb (II), Cu (II), and As (III) with TiO2 nanoparticles. Conversely, during the adsorption process, the first stage exhibited rapid activity, which thereafter began to decrease progressively. The biphasic behavior was likely attributed to the diverse reactive sorption sites or the passage of adsorbate ions onto the adsorbent [13]. TiO2 has satisfactory effectiveness in adsorption; nevertheless, it requires an enhanced reaction rate [14]. TiO2 nanostructures, including nanosheets, nanofibers, nanoflakes, nanowires, and nanoflowers, have garnered significant interest due to their elevated specific surface area and charge-transfer rate, facilitating the efficient removal of pollutants from water effluents [15-16].

The subsequent findings pertain to research advancements in the adsorption domain utilizing one-dimensional TiO2 nanomaterials. Youssef et al. (2014) emphasized the influence of the

adsorption capability of titanium dioxide nanowires (TiO2) on heavy metals including Pb2+, Cu2+, Fe3+, Cd2+, and Zn2+. Extensive investigations on the manufacture of TiO2 nanotubes employing straightforward iodization and wet impregnation methods were conducted to eliminate very toxic BP (II) metal ions. In his investigation, a high dosage of adsorbent was employed to eliminate 25 ppm of lead from the stock solution, which is expected to cause secondary contamination due to excess active sites [18]. Li et al. (2015) delineated the significant benefits of the hydrothermal process compared to template-assisted and electrochemical anodic oxidation procedures, which are regarded as conventional methodologies frequently employed in the creation of annotates. This hydrothermal approach produces a surplus of hydroxyl groups on the surface, which can efficiently trap cations through an ion-exchange process, enhancing the adsorption effect [22]. The straightforward development of innovative adsorbent materials that are cost-effective and have minimal environmental impact is highly significant. Recently, TiO2 nanotubes synthesized with a glycerol-assisted, simple alkaline hydrothermal technique from commercially available TiO2 nanoparticles have proven to be highly cost-effective and straightforward. Consequently, considering the advantages and disadvantages of prior research on the adsorption properties of TiO2, this study focuses on the synthesis of highly active single crystalline one-dimensional TiO2 nanorods by a straightforward hydrothermal process. The synthesized adsorbent was utilized for the extraction of heavy metals, including chromium, lead, and copper ions, in this study. The adsorption mechanism was elucidated by isotherm modeling, specifically employing the Langmuir and Freundlich models.

1.2 Materials

Titanium dioxide powder (TiO_2), sodium hydroxide (NaOH), glycerol($C_3H_8O_3$), hydrochloric acid (HCl, 35%) and ethanol (C_2H_5OH) were purchased from Sigma-Aldrich. All the chemicals wereof analytical grade and used without any further purification.

1.2.1Preparation of TiO_2 Nanorods

In a typical process, TiO_2 nano powder and glycerol were added to 10 M NaOH aqueous solution followed by magnetic stirring for 2 hours. The dispersed solution was autoclaved for hydrothermal treatment at 180 °C for 18 hours. After which, the obtained sample was washed with 0.1 M HCl aqueous solution until pH reachedneutral. Then, the particles were collected by centrifugation with ethanol, followed by drying at 80 °C for 48 hours and finally annealed in air at 380 °C for 4 hours to yield TiO2 nanorods. The schematic representation of the above-mentioned synthesis of TiO_2nanorods is picturized in Fig 3.1.

Fig.3.1.SchematicrepresentationofthesynthesisofTiO2nanorodsusingfacile hydrothermal method

Characterization

The identification of phase and structure of the prepared sample was investigated using X-rayDiffractometer (Bruker D8advance) operated at 40 kVand 30 mA with CuKα radiation (λ =1.5406 Å). FEI Quanta FEG 200 - High Resolution Scanning Electron Microscope coupled

with Energy Dispersive spectrum was used to examine the surface morphology and elemental composition of the sample. Fourier Transform Infrared (FTIR) spectra was recorded using a Perkin-Elmer spectrometer, model (2000), with wave number range from 400 cm^{-1} to 4000 cm^{-1} and Raman spectra was recorded using a micro-Raman spectrometer (Witech CRM 200, the excitation wavelength at 532 nm). The surface electronic states were analyzed by X-ray photoelectron spectroscopy (XPS, Perkin-Elmer PHI 5000 Versa Probe III). The adsorption capacity of the sample was studied using Atomic Adsorption Spectroscopy (AAS).

RESULTSANDDISCUSSION

1.2.3 X-Ray Powder Diffraction (XRD) analysis of TiO2 nanorods

X-ray powder diffraction (XRD) is an analytical technique used to determine the phase of a crystalline material. The crystalline structure of the sample is determined using XRD and is represented in Fig.3.2.The diffraction peaks of TiO_2 located at 2θ=25.1°,36.9°,37.8°,38.44°,47.8°,53.8°,55.0°,62.4°,68.5°,70.4°,75.7°,76°, 82.9°correspondsto (101), (103),(004), (112),(200), (105),(211),(204), (116),(220), (215), (301), (224)planes respectively. The diffraction peaks of $TiO_2$are in good agreement with (JCPDSNO 21-1272) and also the space group is found to be I41/amd. TiO_2 isfoundtoexhibittetragonalstructureandtheaveragecrystallitesizeiscalculated using Deby Scherrer equation (1),

$$D=\frac{K\lambda}{\beta \cos\theta} \text{ ----------(1)}$$

Where, λ is the wavelength of incident radiation, β is the full width at half maximum (FWHM), K is shape factor and θ is the Bragg's angle. Furthermore, the peaksproduced are relatively sharp indicating the high crystalline nature of pure anatase TiO_2nanorods. The crystallite size is calculated to be 36.08 nm and the lattice constants are a= 3.625Å and c = 9.316 Å which corresponds the tetragonal structure [24].

Fig.3.2.XRD pattern of TiO2nanorods

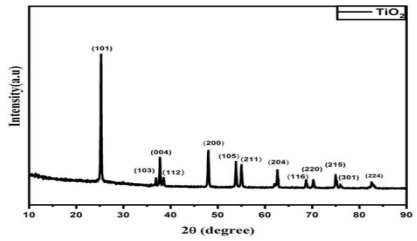

Fourier Transform Infrared Spectroscopy (FTIR) analysis of TiO2nanoparticles

Fourier Transform Infrared (FT-IR) spectroscopy is a beneficial technique for identifying the chemical bonding or molecular structure of materials. The FTIR spectrum of pristine TiO_2nanoparticles is shown in Fig.3.3. The prominent absorption peak at 483 cm^{-1} is the characteristic peak of Ti-O bond. The spectrum also exhibitstwo broad band's centered at 3480 and 1623.50 cm^{-1} referring to the stretching and bending modes of vibrations of physical adsorbed water and the presence of Ti -OH bonding vibration as reported by [25]. The presence of these hydroxyl radicals is absolutely essential for the elimination of pollutants from aqueous medium [26]. The bands displayed at 772 cm^{-1} and 961 cm^{-1}maybe assigned to C-H stretching which can be associated to the presence of glycerol in the sample.

Raman Spectroscopy analysis of TiO2nanorods

To provide better insight into the structure of synthesized TiO_2 nanoparticles Raman spectrum was studied. Six Raman active modes confirm the presence of anatine TiO_2 nanoparticles. 2Bg

and 1Ag respectively. The spectrum in Fig.3.4. clearly demonstrates bands at 144.3 (Eg), 195.7 (Eg), 395.3 (B1g), 513 (A1g), 519 (B1g), and 637.9 cm^{-1} (Eg) which confirms the presence of TiO_2 nanop articles. The Raman result is found to be in good agreement with XRD data and thereby confirmsthe purity of TiO_2 anatase phase which is prepared by the hydrothermal synthesis at moderate temperature. Also, the obtained results are in good correlation with [27].

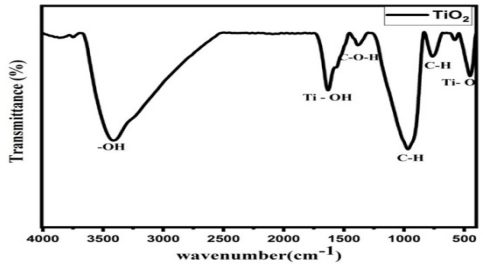

Fig.3.3. FTI Rspectrum of TiO_2 nanorods

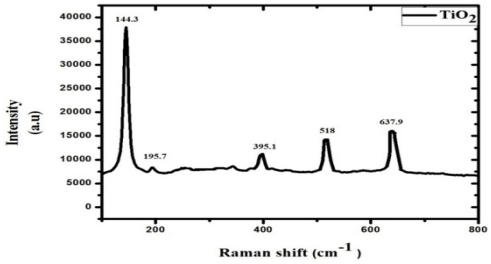

Fig.3.4.Raman Spectroscopy analysis of TiO_2 nanorods

Morphological analysis of TiO_2 nanorods by HR-SEM and EDAX

Microscopic examination is the predominant and most dependable method for directly seeing the surfaces of nanostructures. The sample surface is examined using a High-Resolution Scanning Electron Microscope (HR-SEM), which employs a high-energy electron beam for analysis. The HR-SEM picture in Fig. 3.5a clearly illustrates the production of nanorods with sharp edges. The sample mostly contains one-dimensional TiO_2 nanorods. In comparison to other TiO_2 structures, this nanorod configuration is very intriguing and appears suitable for enhancing active surface interaction with metal ions, hence promoting effective adsorption. Such nano-architectures are particularly advantageous for improving the adsorption effect, as indicated by [28].

The elemental composition of a specimen can be determined by Energy Dispersive X-ray Analysis (EDAX), often referred to as Energy Dispersive X-ray Spectroscopy (EDS). It is commonly utilized alongside imaging instruments like as SEM and TEM to examine surface constituents. Each of these peaks is characteristic of an atom and signifies a certain element. The peak's strength correlates with the chemical makeup of the respective element. The energy dispersive X-ray (EDAX) spectra of the TiO_2 nanorods are illustrated in Fig. 3.5 (b). The EDAX spectra of the samples verify the existence of Ti and O in their corresponding ratios. It confirms that all the nanorods are synthesized without any contaminants.

Fig.3.5.a.)HR-SEMandb) EDAX images of TiO_2 nanorods

High-Resolution Transmission Electron Microscopy (HRTEM) of TiO_2nanoparticles

High Resolution Transmission Electron Microscopy (HRTEM) allows the imaging of the crystallographic structure of the sample even at atomic scale. It can produce atomic-sized

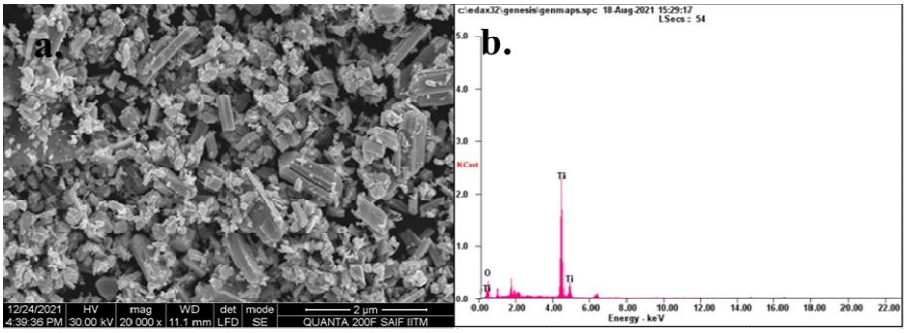

resolution of lattice pictures with a spatial precision of 1 nm or above A comprehensive analysis of the structure and crystallinity of TiO2 nanorods is effectively elucidated by HR-TEM micrographs. Figures 3.6.a) and b) distinctly demonstrate the development of rods in the synthesized sample. Figure 3.6.c) demonstrates that the distinct lattice spacing indicates a significant degree of crystallinity in the nanorods [29]. The nanorods exhibit near-straightness and uniformity across their length and thickness, akin to the elongated TiO2 nanorods reported by [30]. The interplanar spacing of the nanorods may be ascertained by measuring the distance between neighboring lattice fringes. The nanorods have a lattice spacing of d=0.354 nm in the (101) plane, indicating the presence of the anatase phase, and the findings align with the XRD study as well [31]. The Selected Area Electron Diffraction (SAED) pattern of TiO2 nanorods, seen in Fig. 3.6.c), unequivocally validates the single crystalline character of the sample. Consequently, nanorods with a substantial surface area and many active sites, which are very advantageous for the adsorption of pharmaceuticals, are produced, representing the primary objective of this research.

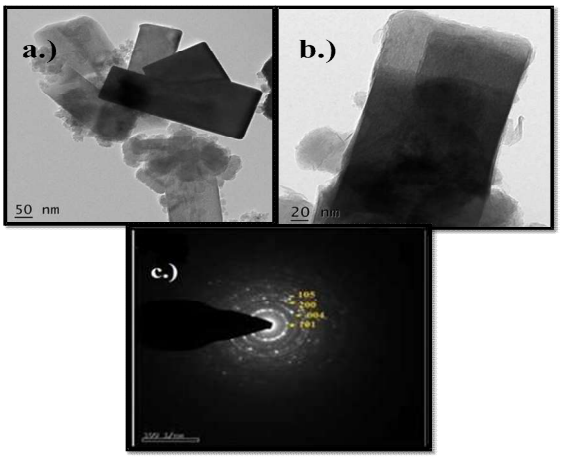

Fig.3.6.(a,b)HR-TEM and c.)SAED images of TiO2 nnaorods

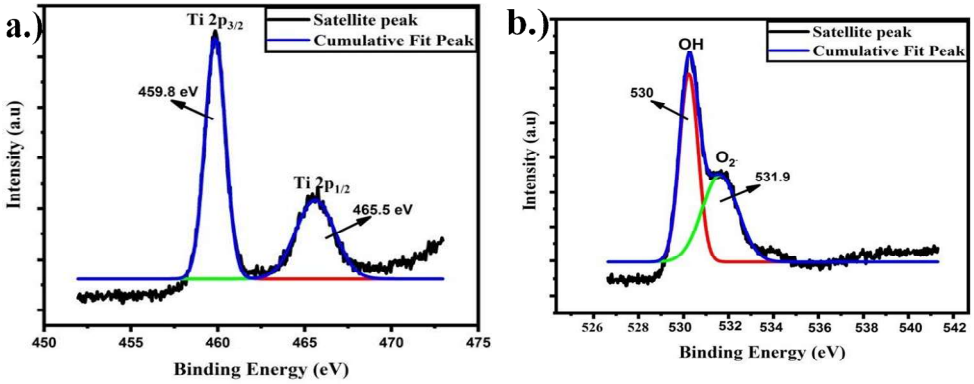

X-ray Photo electron

Spectroscopy (XPS) analysis of TiO2nanorods

XPS is a surface analysis technique which provides detailed description of oxidation states of cations present in the sample. Fig.3.7. depicts distinct photoelectron peaks forTi 2p and O1s peaks. TheTi 2p is deconvoluted into two characteristicpeaks such as 459.8 eV and 465.5 eV which corresponds to Ti 2p3/2 and Ti 2p1/2of Ti^{4+} in TiO2. The O 1s is deconvoluted into 531.3eV and 533.4 eV which represents two oxygen chemical states. The main contribution of nano adsorbent is attributed to O and the rpeakisal locatedto OH present on the surface of the nanoads orbent .S.G. Ullattil et al. (2018) reported a similar trend, with Ti mesh samples exhibiting characteristic peaks at 529.9 eV and 532.0 eV referring to Ti-O-Ti bond and Ti-OH respectively. A comparison table of TiO2 based adsorbents with adsorption capacity value or removal efficiency is presented in Table.3.2.

Batch experiments were conducted to determine the effect of TiO2for the adsorption of lead, copper and chromium ions. The adsorbent dosage was added into 500 ppm of heavy metal solution. The required solution was continuously agitated using so phisticated copper stirrer equipment for various time intervals such as 2, 4, 6,8 and24hoursatnormalroomtemperature. The samples were complete lyre move dousing a ready to use nylon filter syringe with pore size of 0.22 μm and diameter 25 mm and then analyzed for Atomic Adsorption Spectroscopy (AAS) experiment.

Table.3.2.AcomparisontableofTiO2basednanoadsorbentsfortheelimination of heavy metals

Nanomaterial	Pollutant	Removal Efficiency (%)	Adsorption Capacity (Mg/L)	Pollutant
TiO2-immobilized mesoporous MCM-41	Cr (VI)	91	-	[Paridaetal. (2012)]
flyashcoatedwith TiO2	Cu(II) Cd(II)	84.7 80	-	[Visaet al. (2013)]
TiO2	As(V) As(III)	-	4.05 3.93	[Jingat al. (2009)]
TiO2	As(III)	60	-	[Luoetal. (2010)]
TiO2	Pb(II) Cd(II) Ni (II)	100 99 99	-	[Engatesetal. (2011)]
TiO2	Zn(II) Cd(II)	--	15.3 7.9	[Liangetal. (2004)]
nano-TiO2	Pb(II)	-	7.41	[Poursanietal. (2016)]
Anatasenano-TiO2	Cu(II) Pb(II) As(III)	--	31.25 23.74 16.95	[Z.Özlemet al. (2013)]
Cudoped TiO2 nanotube	Pb(II)	79.5	-	[S.Sreekantan etal. (2014)]
Titanate nanotubes	As(V) As(III)	--	204.1 59.5	[H.Y. Niu et al.(2009)]
Anatase-type titanium dioxide	Cu(II)	-	8.415	[M.-S.Kim et al.(2003)]
Hydrous titanium(IV)oxide	Ni(II)	47.8	-	[S.Debnathet al.(2009)]
nano-TiO2	Hg(II)	96	-	[Z. Ghasemi etal. (2012)]

The adsorption capacity and removal efficiency of the adsorbent were determined using the formulae:

$$q_e = \frac{V(C_0 - C_e)}{W} \text{----------(2)}$$

$$R = \frac{(C_0 - C_e)}{C_0} \times 100\% \text{----------(3)}$$

Where, $q_e$is the amount of adsorbed metal (mg/g), R is the removal efficiency, $C_0$is the concentration of initial adsorb ate (mg/L), $C_e$is the adsorb ate concentration at equilibrium (mg/L), $C_f$is the final adsorb ate concentration, V is the volume of the adsorb ate(L),Was the mass of the a adsorbent (mg).There movable efficiency of TiO_2 was calculated as 77.6%, 84.5% and 86.77 % for lead, chromium and copper metal ions for a maximum time interval of12 hours.Fig3.8. shows the increase of removal efficiency with increase in time interval.

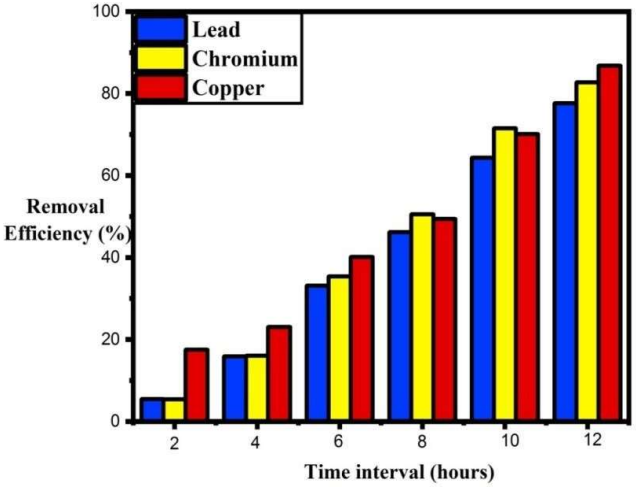

Fig.3.8. Removal Efficiency of heavy metal pollutants

This adsorption phenomenon is mainly attributed due to the complication of functional groups and through ion exchange mechanism. The complication of adsorbent and adsorb ate (oxyanion) is as follows,

$$2ROH^-(s) + M^{2+}(aq) \longleftrightarrow [(RO^-)2M^{2+}](s) + 2H^+$$

$$2RCOO^-(s) + M^{2+}(aq) \longleftrightarrow [(RCOO^-)2M^{2+}](s)$$

Where R indicates the surface of adsorbent and M indicates metal ions. This is also attributed to the intrinsic factors which correspond to the selectivity of adsorbent and extrinsic factors like pH, temperature, nanoparticles loading and concentration of heavy metals.

For the regeneration experiment the utilized adsorbent was treated with 0.5-M NaOH solution under agitation for 6 hours, washed, dried and finally used for the next cycle of the adsorption processes. The sample demonstrated consistent regeneration efficiency for three cycles which proved its potentialst ability for water treatment as can be seen from the graphing Fig.3.9.A slight decrease in the adsorption capacity was also encountered which coincides with the regeneration results asobtainedby [33].

Fig.3.9. Regeneration experiment of TiO_2 adsorbent

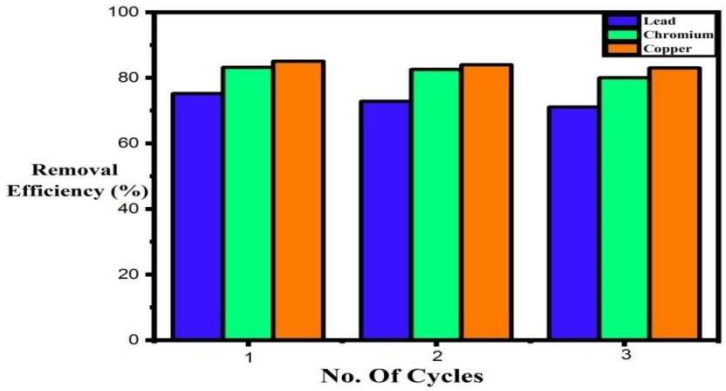

The adsorption mechanism can be explained using sorption isotherm modelling which provides a deeper understanding of how metal ions interact with the active spots on the sorbent surface. The isotherm data are fitted using Langmuir and Freundlich isotherms and is presented in Fig.3.10. Langmuir isotherms concept is that sorption is due to monolayer possessing independent equivalent active sites.

$$q_e = \frac{V K_L q_m C_e}{1+KC} \text{----------(4)}$$

Where, $C_e$represents the equilibrium concentration (mg/L), q_e and $q_m$is the quantity adsorbed at equilibrium (mg/g) and maximum adsorption capacity respectively. $K_L$is the Langmuir constant (L/ mg).Theabove equation (5)canberearranged tothefollowinglinear form:

$$\mathbf{C_e/q_e = 1/K_L q_m + C_e/q_m} \text{----------(5)}$$

The high affinity of TiO_2towards metal ions developed multi-layered complexes of surface functional groups for the remediation process. These available active sites shortened the equilibrium level and increased the driving force and finally hastened the adsorption reaction.

The Freundlich isotherm is an empirical model that assumes different sites with several adsorption energies involved on a heterogeneous surface [34].The Freundlich equation can be written as:

$$\mathbf{\log q_e = \log K_F 1/n + \log C_e} \text{----------(6)}$$

Where $K_F$and n are Freundlich isotherm constants (mg/ L) and constant related to the surface of adsorption respectively. This can be determined from plot log $q_e$vs. log Ce.

It was found that the adsorption of Pb (II), Cr (VI) and Cu (II) on nano-$TiO_2$was correlated for Langmuir and Freundlich isotherm modelling. The R^2 valuessuch as 0.9841, 0.99530, 0.99712 from Langmuir equation was compared with the R^2values of Freundlich equation corresponding to 0.87104, 0.84290, 0.8639. Langmuir isotherm fitting is found to be better than Freundlich isotherm in all conditions according to the correlation coefficients obtained and presented in table 3.3 a.), b.) and c.). Therefore, the results suggested that the adsorption process was due to the homogeneous surfaceofTiO_2 nanoparticles.

Table3.3.a.)AASparameterscalculatedfortheremovalofleadionsusingTiO_2at different time intervals

HRS	C0	Ce	Qe	Ce/qe	Log Ce	Logqe	Removal Efficiency (%)	R^2 Langmuir	R^2 Frendluich
2	0.9	0.85	0.08	10.4	-0.07	-1.08	5.44		
4	0.9	0.75	0.08	8.47	-0.12	-1.04	15.88		
6	0.9	0.60	0.09	6.02	-0.22	-1.00	33.11	0.9841	0.87104
8	0.9	0.48	0.12	3.94	-0.31	-0.91	46.22		
10	0.9	0.32	0.20	1.60	-0.49	-0.69	64.44		
12	0.9	0.20	2.55	0.07	-0.69	-0.40	77.64		

Table3.3.b.)AASparameterscalculatedfortheremovalof chromiumionsusing TiO_2 at different time intervals

HRS	C0	Ce	Qe	Ce/qe	Log Ce	Logqe	Removal Efficiency (%)	R^2Langmuir	R^2 Frendluich
2	0.9	0.90	0.07	11.3	-0.04	-1.10	5.46		
4	0.9	0.79	0.08	8.92	-0.09	-1.04	17.01		
6	0.9	0.61	0.10	5.82	-0.21	-0.97	35.92	0.9953	0.84290
8	0.9	0.47	0.15	3.09	-0.32	-0.81	50.63		
10	0.9	0.27	1.36	0.19	-0.56	-0.13	71.53		
12	0.9	0.16	0.78	0.20	-0.78	-0.10	82.75		

Table3.3.c.) AASpara meters calculated for there moval of chromium ions using TiO2 at different time intervals

HRS	C0	Ce	Qe	Ce/qe	Log Ce	Logqe	Removal Efficiency (%)	R^2 Langmuir	R^2 Frendluich
2	0.85	0.70	0.14	4.70	-0.15	-0.82	17.52		
4	0.85	0.65	0.19	3.33	-0.18	-0.70	23.05		
6	0.85	0.50	0.34	1.49	-0.29	-0.46	40.11	0.9971	0.863
8	0.85	0.43	0.42	1.02	-0.36	-0.37	49.41		
10	0.85	0.25	0.59	0.42	-0.59	-0.22	70.11		
12	0.85	0.11	0.73	0.15	-0.95	-0.13	86.82		

Fig.3.10.Langmuir and Frendluichi so ther mmodeling a andb) for lead, candd) for Conclusion

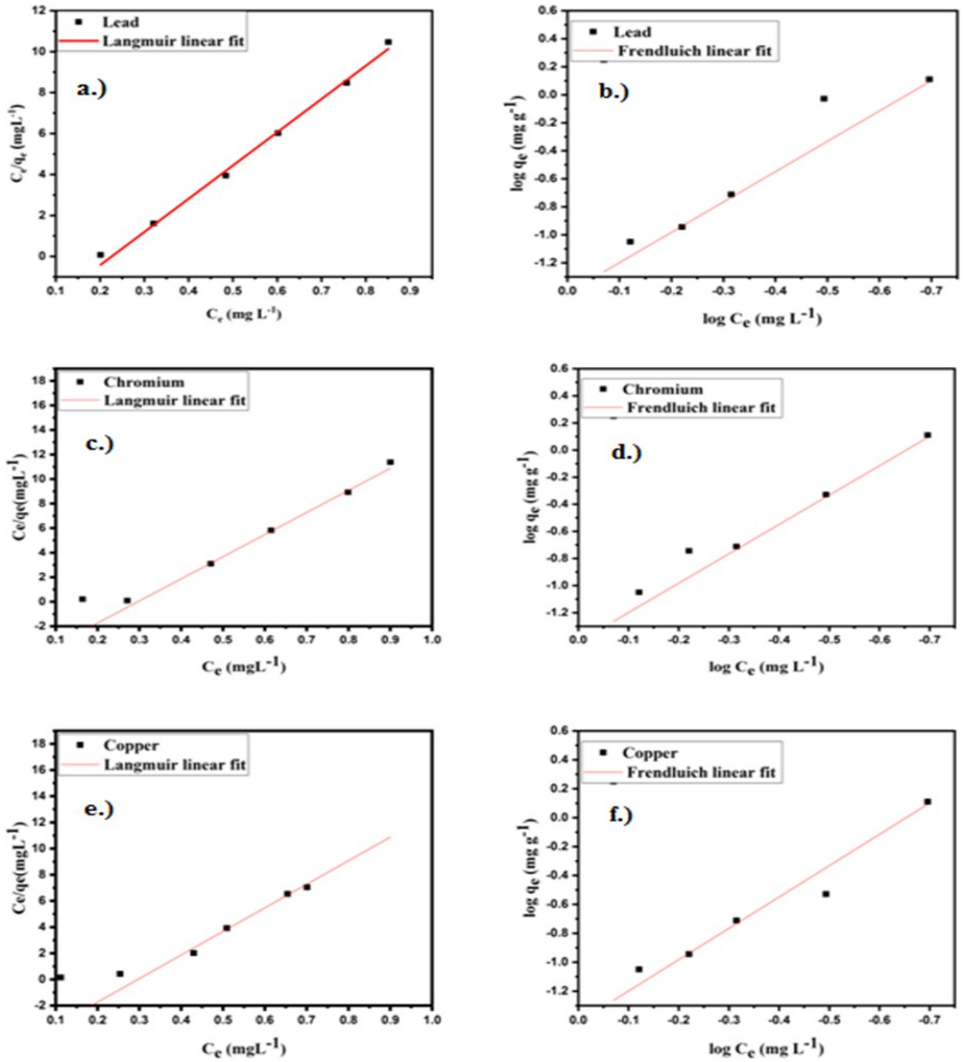

A summary of the studyof TiO2 nanorods preparation and it suseinremediation XRD confirmed a pure crystalline TiO2 nanoparticles fabricated using facile and economical hydrothermal method. HR-SEM –EDAX, HR-TEM images confirmed the one-dimensional rod- like morphology and the EDAX study confirmed the elemental composition associated with pure TiO2 nanoparticles. FT-IR and Raman studies provided information on the functional groups and stretching modes which are attributed to TiO2. AAS technique revealed that the large

active sites are found to play a crucial role in the adsorption of inorganic pollutants such as lead, chromium and copper metal ions. The removal efficiency was calculated as 77.6%, 82.75% and 86.82 % for lead, chromium and copper metal ions respectively for 12 hours of time intervals. The isotherm modeling explains monolayer adsorption mechanism for TiO_2nanorods which are found to be well correlated with the other research reports.

Reference

1. Ahmed, M. A. (2012). *Journal of Photochemistry and Photobiology A: Chemistry, 238*, 63–70.
2. Barakat, M. A. (2005). *Journal of Colloid and Interface Science, 291*(2), 345–352.
3. Chen, H. (2018). *International Journal of Electrochemical Science, 13*(2), 2118–2125.
4. Choi, W., Kim, S., Cho, S., Yoo, H. I., & Kim, M. H. (2001). *Korean Journal of Chemical Engineering, 18*(6), 898–902.
5. Dai, S., Wu, Y., Sakai, T., Du, Z., Sakai, H., & Abe, M. (2010). *Nanoscale Research Letters, 5*(11), 1829–1835.
6. Devi, L. G., Kottam, N., Murthy, B. N., & Kumar, S. G. (2010). *Journal of Molecular Catalysis A: Chemical, 328*(1-2), 44–52.
7. Du, J., Chen, H., Yang, H., Sang, R., Qian, Y., Li, Y., Zhu, G., Mao, Y., He, W., & Kang, D. J. (2013). *Microporous and Mesoporous Materials, 182*, 87–94.
8. Geng, Q., & Cui, W. (2010). *Industrial & Engineering Chemistry Research, 49*(22), 11321–11330.
9. Ghasemi, Z., Seif, A., Ahmadi, T. S., Zargar, B., Rashidi, F., & Rouzbahani, G. M. (2012). *Advanced Powder Technology, 23*(2), 148–156.
10. Hafez, H. S. (2009). *Materials Letters, 63*(17), 1471–1474.
11. Hu, J., & Shipley, H. J. (2013). Regeneration of spent TiO_2 nanoparticles for Pb(II), Cu(II), and Zn(II) removal. *Environmental Science and Pollution Research, 20*(8), 5125–5137.
12. Jung, J. H., Kobayashi, H., van Bommel, K. J. C., Shinkai, S., & Shimizu, T. (2002). *Chemistry of Materials, 14*(4), 1445–1447.
13. Kabra, K., Chaudhary, R., & Sawhney, R. L. (2007). *Journal of Hazardous Materials, 149*(3), 680–685.
14. Kim, M.-S., Hong, K.-M., & Chung, J. G. (2003). *Water Research, 37*(14), 3524–3529.
15. Kocabaş-Ataklı, Z. Ö., & Yürüm, Y. (2013). *Chemical Engineering Journal, 225*, 625–635.
16. Li, X., Liu, W., & Ni, J. (2015). *Microporous and Mesoporous Materials, 213*, 40–47.
17. Manzoori, J. L., Amjadi, M., & Hallaj, T. (2009). *International Journal of Environmental Analytical Chemistry, 89*, 749–758.
18. Raven, K. P., Jain, A., & Loeppert, R. H. (1998). *Environmental Science & Technology, 32*(3), 344–349.
19. Santhi, K., Navaneethan, M., Harish, S., Ponnusamy, S., & Muthamizhchelvan, C. (2020). *Applied Surface Science, 500*, 144058.
20. Smith, K. A., Savva, A. I., Mao, K. S., Wang, Y., Tenne, D. A., Chen, D., Liu, Y., et al. (2019). *Journal of Materials Science, 54*(20), 13221–13235.
21. Sreekantan, S., Zaki, S. M., Lai, C. W., & Tzu, T. W. (2014). Copper-incorporated titania nanotubes for effective lead removal.
22. Sun, H., Zhang, X., Niu, Q., Chen, Y., & Crittenden, J. C. (2007). *Water, Air, and Soil Pollution, 178*(1–4), 245–254.
23. Tian, J., Zhao, Z., Kumar, A., Boughton, R. I., & Liu, H. (2014). *Chemical Society Reviews, 43*(20), 6920–6937.
24. Ullattil, S. G., Narendranath, S. B., Pillai, S. C., & Periyat, P. (2018). Black TiO_2 nanomaterials.
25. Wang, T., Liu, W., Xiong, L., Xu, N., & Ni, J. (2013). *Chemical Engineering Journal, 215*(e216), 366–374.
26. Yacoub, N., Ramadan, A. R., & Ragai, J. (2005). *Adsorption Science & Technology, 23*(3), 215–224.
27. Youssef, A. M., & Malhat, F. M. (2014). *Macromolecular Symposia, 337*(1), 96–101.
28. Yuan, Z. Y., & Su, B. L. (2004). *Colloids and Surfaces A: Physicochemical and Engineering Aspects, 241*(1–3), 173–183.
29. Zhao, P., Wu, W., Zhang, Q., Jin, R.-B., Xu, Y. L., & Goto, T. (2018). *Thin Solid Films, 662*, 33–40